Published in final edited form as:
Chembiochem. 2010 July 5; 11(10): 1458–1466. doi:10.1002/cbic.201000070.

Evolved Diversification of a Modular Natural Product Pathway: Apratoxins F and G, Two Cytotoxic Cyclic Depsipeptides from a Palmyra Collection of *Lyngbya bouillonii*

Dr. Kevin Tidgewell[a], **Niclas Engene**[a], **Tara Byrum**[a], **Joseph Media**[b], **Dr. Takayuki Doi**[c], **Dr. Fred A. Valeriote**[b], and **Dr. William H. Gerwick**[a]

William H. Gerwick: wgerwick@ucsd.edu

[a]Scripps Institute of Oceanography, CMBB, University of California, San Diego, 9500 Gilman Dr., La Jolla, CA 92093-0212, Fax: (858_534-0529

[b]Henry Ford Health System, Department of Internal Medicine, Josephine Ford Cancer Center, 440 Burroughs, Room 415, Detroit, MI 48202

[c]Graduate School of Pharmaceutical Sciences, Tohoku University, 6-3 Aza Aoba, Aramaki, Aoba-ku, Sendai 980-8578, Japan

Abstract

A collection of Lyngbya bouillonii from Palmyra Atoll in the Central Pacific, a site several thousand kilometers distant from all previous collections of this chemically prolific species of cyanobacterium, was found to contain two new cancer cell cytotoxins of the apratoxin family. The structures of the new compounds, apratoxins F and G, were determined by 1-D and 2-D NMR techniques in combination with mass spectrometric methods. Stereochemistry was explored using chromatographic analyses of the hydrolytically released fragments in combination with NMR and optical rotation comparisons with known members of the apratoxin family. Apratoxins F and G add fresh insights into the SAR of this family because they incorporate an N-methyl alanine residue at a position where all prior apratoxins have possessed a proline unit, yet they retain high potency as cytotoxins to H-460 cancer cells with IC_{50} values of 2 and 14 nM, respectively. Additional assays using zone inhibition of cancer cells and clonogenic cells give a comparison of the activities of apratoxin F to apratoxin A. Additionally, the clonogenic studies in combination with MTD studies provided insights as to dosing schedules that should be used for in vivo studies, and preliminary in vivo evaluation validated the predicted in vivo efficacy for apratoxin A. These new apratoxins are illustrative of a mechanism, the modification of an NRPS adenylation domain specificity pocket, for evolving a biosynthetic pathway so as to diversify the suite of expressed secondary metabolites.

Keywords

Natural Products; Structure Elucidation; Anti-Cancer; Structure-Activity Relationships; Cyanobacteria

Correspondence to: William H. Gerwick, wgerwick@ucsd.edu.

Supporting information for this article is available on the WWW under http://www.chemmedchem.org or from the author.

Introduction

Modular NRPS and PKS biosynthetic pathways are especially well suited to pathway diversification in that small changes in one module can incrementally modify appendages on a structural framework,[1] a logic of structural exploration familiar from the fields of medicinal and combinatorial chemistry. Marine cyanobacteria are especially well endowed with these types of modular biosynthetic pathways which they employ to produce a rich arsenal of bioactive secondary metabolites.[2,3] For example, the apratoxin family of depsipeptides are exquisitely potent cytotoxins with the parent structure, apratoxin A (**1**), showing subnanomolar cytotoxicity to several different cancer cell lines in vitro.[4] Unfortunately, in evaluating apratoxin A for in vivo anticancer activity, it showed limited or no activity against tumors (colon and breast) at sub-lethal doses, and at higher doses, animal toxicity and weight loss were observed.[4] As discussed here, this lack of therapeutic efficacy could be a consequence of a non-optimal dosing schedule.

Two additional apratoxins B (**2**) and C (**3**), simple desmethyl analogs of apratoxin A, were subsequently isolated from collections of *Lyngbya sp.* made in Guam and Palau in 2002,[5] and in 2008, our group reported apratoxin D (**4**) from collections of *Lyngbya sordida* and *Lyngbya majuscula* along with apratoxins A-C from a collection of *Lyngbya bouillonii* made in Papua New Guinea.[6] This fourth apratoxin analog, apratoxin D, possessed a new carbon skeleton which appears to result from an additional PKS element in the biosynthetic pathway. Also in 2008, the Luesch group reported apratoxin E (**5**) from a collection of *Lyngbya bouillonii* made in Guam, an analog with several changes to the decorated structure of apratoxin A.[7]

Due to the potent cytotoxic activity, anticancer potential, and novel carbon skeleton of apratoxin A, several total syntheses have been reported.[8–12] Several of these efforts have focused on production of analogs so as to develop further structure activity relationship (SAR) knowledge in this metabolite class.[9–15] To date, these investigations, coupled with the reported natural products apratoxins A–E (**1**–**5**) and our report here of apratoxins F (**6**) and G (**7**), indicate that several disparate regions of the molecule are important for maximal biological activity, however, that the connected lower regions from C-39 to the t-butyl terminus and C-1 to C-5 are more tolerant of structural changes (Scheme 1).

A functional genomics approach was used to gain an initial understanding of the mechanism of action of apratoxin A, and revealed that the drug induces a G1-phase cell cycle arrest and apoptosis via interaction with STAT3 and FGFR signaling.[16] Further studies determined that the inhibition of STAT phosphorylation is caused by down regulation of an IL-6 transducer and several cancer specific receptor tyrosine kinases. These alterations result in prevention of the translocation of several proteins involved in the secretory pathway and is reversible in normal cells but not in cancer cells.[17] Interestingly, a separate study showed that the oxazoline analog of apratoxin A interacts with Hsp90, a well known and important cancer cell target.[18]

The combination of potent cytotoxic activity with selectivity for cancer cells, a unique mechanism of action, and a novel structural framework, make the apratoxins an exciting molecular class for potential development as chemotherapeutic agents. Thus, the characterization of new naturally occurring apratoxins which further refine SAR in this molecular class is important. Moreover, as the biosynthesis of the apratoxins becomes clarified, it is insightful to consider how the pathway has evolved to produce and modulate the unique structural features present in the different apratoxins.[19] Principal among these is a tertiary butyl group as the presumed starter group for the entire pathway, a completely reduced beta-branch carbon similar to that found in the curacins and jamaicamides,[20] an

interdigitated NRPS/PKS architecture, and a 25-membered ring presumably produced concurrent to off-loading from an NRPS catalyst. With the possibility of isolating new active analogs of the apratoxin structural class we collected samples of *Lyngbya bouillonii* from Palmyra Atoll, a site more than 3200 km from all prior collections of the cyanobacterium. Indeed, upon cancer cell toxicity guided isolation and spectrochemical structure elucidation, this geographically distant sample of *Lyngbya bouillonii* yielded two novel and highly bioactive natural products in this structure class, apratoxins F (**6**) and G (**7**), which we report herein.

Results and Discussion

Palmyra Atoll, approximately 1500 km south-southwest of Honolulu, is an unincorporated territory of the United States that is jointly overseen by the Fish and Wildlife Service, The Nature Conservancy, and a Palmyra Atoll Research Consortium (PARC).(http://www.palmyraresearch.org/) Its remote location as one of the northernmost Line Islands contributes to its rich abundance of aquatic wildlife. In 2008, we collected tube-like colonies of the deep red-pigmented cyanobacterium *Lyngbya bouillonii* (collection code PAL08-16) from reefs 9–15 m deep.[21] Elsewhere in the South and Indo Pacific regions (e.g. Papua New Guinea), *L. bouillonii* appears more as a sheet-like morphology; however, in both cases the snapping shrimp (*Alpheus cf. frontalis*) lives in association with the cyanobacterium and is believed responsible for the overt appearance of these colonies. Microscopically, the cyanobacterial filaments were long (1–3 cm), cylindrical, reddish, and slightly waved. The filaments were 26.3 ± 2.3 μm (n = 3) wide and were enclosed with thick and distinct sheaths. Several of the filaments contained hormogonia separated by necridic cells. The vegetative cells were discoid, but relatively long [7.4 ± 1.3 μm long; 24.5 ± 1.8 μm wide; cell width/length ratio = 0.3 (n = 30)]. The vegetative cells were evenly granulated and their cross-walls were distinctly constricted. The terminal cells were rounded and lacked calyptras or thickened cell walls. The cyanobacterium was collected by hand and preserved in EtOH at low temperature until extraction with CH_2Cl_2/MeOH. The extract was subjected to H-460 cancer cell bioassay guided isolation using first NP Vacuum Liquid Chromatography followed by two rounds of RP-HPLC, and yielded **6** and **7** as the active constituents.

By a combination of LC-ESI-MS (obs. [M+H]+ *m/z* 828.30) and HR-ESIMS (obs. [M+Na] + *m/z* 850.4800), the molecular formula of apratoxin F (**6**) was determined as $C_{44}H_{69}N_5O_8S$, hence differing from apratoxin A (**1**) by a single carbon atom and therefore of one less degree of unsaturation. A series of diagnostic NMR signals were highly similar to those reported for apratoxin A (**1**).[4] Notably, all resonances for the two polyketide chain sections of apratoxin A, including the signature *t*-butyl group, were present with minimal chemical shift differences in the spectrum of **6** (Figure 1). The spin systems and associated ^1H and ^{13}C NMR resonances for four of the five amino acids of apratoxin A, namely Cys(thiazoline), *O*-methyl tyrosine, *N*-methyl alanine, and *N*-methyl isoleucine, were also nearly identical to those in apratoxin F. Hence, our structure elucidation efforts focused on identification of the final amino acid residue in all cases heretofore, present as an L-proline residue. Unlike **1**, compound **6** possessed a deshielded alpha proton at δ4.47 which was a quartet (J = 7.5 Hz) and coupled exclusively to a doublet methyl group at δ1.44. HMBC from the alpha proton at δ4.47 also identified an associated carbonyl at δ173.6. A distinctive *N*-methyl group was located at δ3.27 and also showed HMBC correlations to the α-carbon (δ54.4) of this residue, thus defining a second *N*-methyl alanine residue in apratoxin F. Finally, the position of this new residue as a replacement for the proline in apratoxin A was shown by HMBC between the α-hydroxy proton at C-39 (δ4.88) and the carbonyl of this second *N*-Me Ala residue. Similarly, inter-residue HMBC correlations between α-protons and amide carbonyls were used to show an identical linkage

between the other residues in **6** to those in **1**, and thus completed the planar structure of this new member of the apratoxin family (Table 1).

By a combination of LC-ESI-MS (obs. [M+H]+ *m/z* 814.30) and HR-ESIMS (obs. [M+H]+ *m/z* 814.4782), the molecular formula of apratoxin G (**7**) was determined as $C_{43}H_{67}N_5O_8S$, hence differing from apratoxin F (**6**) by a single methylene unit. In a similar manner to **6**, the spin systems and associated ^1H and ^{13}C NMR resonances for four of the five amino acids of **6**, namely Cys(thiazoline), *O*-methyl tyrosine, and two *N*-methyl alanines were also nearly identical in **7**. The final residue was shown to be *N*-Me-Val by the presence of doublet methyl signals at δ0.72 and δ0.95 and the loss of the doublet signal at δ0.92 along with the multiplet signals at δ0.96, and δ1.3. This change from *N*-Me-Ile to *N*-Me-Val accounts for the reduction by a CH_2 in the molecular formula determined by HR-MS. Linkage of the amino acid residues was confirmed to be identical to previous apratoxins based on HMBC correlations.

Configurations of compounds **6** and **7** was determined using a combination of techniques, including ^1H and ^{13}C NMR chemical shift comparisons with the known apratoxins, acid hydrolysis followed by Marfey's analysis, and overall optical rotation. First, the relative configuration of the comparable chiral centers around the macrocyclic ring could be assigned as the same as in apratoxin A based of the similarity of ^1H and ^{13}C NMR chemical shifts and coupling constants (see Supporting Information). Acid hydrolysis of both apratoxins F (**6**) and G (**7**) followed by Marfey's analysis confirmed the presence and stereochemistry of the three amino acids present in both compounds. Fragments from **6** showed retention times of 22.54, 32.51, 34.60 with masses corresponding to *N*-Me-Ala, *O*-Me-Tyr and *N*-Me-Ile, respectively. By contrast, fragments from **7** showed retention times of 22.57, 31.36, and 32.53 with masses corresponding to *N*-Me-Ala, *N*-Me-Val and *O*-Me-Tyr, respectively. Pure samples of the constituent amino acids where derivatized and analyzed in the same manner with retention times of: D-*O*-Me-Tyr (28.00 min), L-*O*-Me-Tyr (32.57 min), D-*N*-Me-Ala (21.85 min), L-*N*-Me-Ala (22.15 min), D-*N*-Me-Ile (30.05 min), D-allo-*N*-Me-Ile (30.40 min), L-*N*-Me-Ile (34.59 min), L-allo-*N*-Me-Ile (34.95 min), D-*N*-Me-Val (27.34 min), L-*N*-Me-Val (31.31 min). By this analysis, **6** was shown to contain L-*N*-Me-Ala, L-*O*-Me-Tyr, and L-*N*-Me-Ile while **7** was shown to contain L-*N*-Me-Ala, L-*O*-Me-Tyr, and L-*N*-Me-Val. Finally, because the optical rotations of **6** and **7** are both large and negative (**6**, $[\alpha]_D$ -249; **7**, $[\alpha]_D$ -206) and the optical rotation of apratoxin A (1) is of similar sign and magnitude ($[\alpha]_D$ -161), they are likely all of the same enantiomeric series.

As a result of this bioassay guided isolation process, two new apratoxins were identified as the major cancer cell and brine shrimp toxins of this Palmyra collection of *L. bouillonii*. In the brine shrimp toxicity assay[22] extract fraction H, containing **6** and **7**, showed 98% toxicity at 1 ppm. In the H-460 cancer cell assay,[23] the IC_{50} value for apratoxin F was 2 nM and for apratoxin G was 14 nM, respectively. For HCT-116 cells, the IC_{50} values for apratoxin A was 1 ng/ml (1.21 nM) and for apratoxin F was 31 ng/ml (36.7 nM). There was insufficient apratoxin G to test against HCT-116, however, it was less potent that apratoxin F as a mixture of apratoxin F and G yielded an IC_{50} value of 120 ng/mL against HCT-116 cells.

Zone inhibition disc assays were conducted with **1** and **6** as previously described[24] against an array of cancer cell lines and a normal cell line (Table 2). For comparable zones, apratoxin F was about 10-fold less potent than for apratoxin A, however, both demonstrated solid tumor selectivity against both human tumor cell lines, HCT-116 and H125. Selectivity is noted by a zone differential ≥250 units between the solid tumor and leukemia (CEM) cells.

A clonogenic concentration-survival study was conducted for **1** and **6** to both define the effect of exposure duration on cytotoxicity and to provide a guide for determining the most effective dose schedule for therapeutic assessment.[24] The clonogenic survival of HCT-116 cells was determined at three different exposure durations: 2 h, 24 h, and continuous (168 h or 7 day), as a function of drug concentration. (Figure 1). The concentration for an exposure duration (t) that yields a surviving fraction of 10% ($_tS_{10}$) was determined: $_2S_{10}$ and $_{24}S_{10}$ for both apratoxin A (Figure 1A) and apratoxin F (Figure 1B) $\gg$ 1.2 μM. For $_{168}S_{10}$ the values were 1.6 and 30 nM, respectively. These results indicate that in order to observe a therapeutic effect with HCT-116 cells in vivo, the concentration of these apratoxins would have to be maintained chronically above either 1.6 or 30 nM, respectively.

A preliminary value for the maximum tolerated dose for apratoxin A in C57Bl/6 mice was found to be between 12.5 μg and 25 μg per mouse daily for 5 days. This dose of 12.5 μg per mouse was then used to perform a study of the therapeutic efficacy of apratoxin A for HCT-116 human colon cancer in SCID mice. The results in Figure 2 show that the tumor in untreated mice becomes detectable about 8 days after implantation and progressively increases in size from that point on until they were sacrificed, at which time the tumor reached 1,000 mm^3. Treatment with 12.5 μg apratoxin A per mouse daily for 5 days beginning on day 0 (3 days after subcutaneous tumor implantation) significantly slowed the rate of tumor size increase. The size of tumors in the treated mice was only 20% of that of the control mice at 22 days (T/C =20%), and is considered to be a good level of therapeutic effectiveness. Unfortunately, four out of the five tumor bearing mice died from drug toxicity at the time points indicated by stars in figure 2.

As noted above, a previous evaluation using a single bolus injection of the maximum tolerated dose of apratoxin A (**1**) in conventional mice bearing syngeneic solid tumors demonstrated little or no therapeutic effect.[4] In our preliminary studies with synthetic apratoxin A using conventional mice, we obtained a similar MTD with the daily x 5 schedule as with the bolus schedule. When we used this dose in SCID mice bearing human tumors and a daily x 5 schedule, we obtained a significant therapeutic effect; however, we also observed significant toxicity. This is not unusual as we have previously shown that SCID mice are more sensitive to a number of chemotherapeutic agents compared to conventional mice[25]; apparently this is also the case for apratoxin A. Regardless, a therapeutic effect was noted against HCT-116 human colon cancer in SCID mice at a dose and schedule of apratoxin A (**1**) that is achievable at or below the MTD in conventional mice, hence validating the predictions from our clonogenic assay.

Current understanding of the SAR of the apratoxin family results from data obtained for both the natural products as well as synthetic and semi-synthetic analogs (Figure 3). Briefly, compared to apratoxin A (**1**), apratoxin B (**2**) lacks the isoleucine *N*-methyl group (30 to 40-fold loss), apratoxin C (**3**) possesses an isopropyl starter unit (2-fold loss), (*E*)-34,35-dehydro-apratoxin A is a semi-synthetic derivative of apratoxin A, (72-230 fold loss), apratoxin D (**4**) has an extended *t*-butyl starter unit (roughly equivalent activity), and apratoxin E (**5**) has three modifications including a (*Z*)-34,35-dehydration, loss of the *C*-28 methyl group and saturation of the *C*-28/29 bond (only a modest loss of activity). From synthetic approaches, it was discovered that replacement of the sulfur in the thiazole ring with an oxygen to create an oxazole was tolerated,[11] a modification which may facilitate the production of a library of oxoapratoxin analogs by solid phase total synthesis.[15] The *C*-37 methyl group in the polyketide section has been shown to be required, and that its stereochemistry is important to the biological activity.[7] While the *C*-34 methyl group has also been examined by synthetic approaches, the biological effect of alterations in its configuration has not yet been reported.[12]

Hence, apratoxins F (**6**) and G (**7**) are the first apratoxin analogs to probe the biological consequence of modifications in the peptidic portion of the apratoxin skeleton, specifically, the biosynthetically-terminating proline residue. Somewhat remarkably, despite the fact that all natural and synthetic analogs reported to date possess a proline residue at this position, these new apratoxins reveal that this is not a required feature of the molecule. A consequence of this replacement in **6** and **7** is a loss of rigidity in the lower section of the molecule, thus allowing for some greater conformational flexibility in these new analogs. Additionally, **7** shows that exchange of the *N*-methyl isoleucine with an *N*-methyl valine causes a 7-fold reduction in activity compared to **6**. Overall, a picture is beginning to emerge wherein features of the Eastern and Northern portions of the molecule are quite critical for activity, while the Southern section seems quite tolerant of change. Except for modifications to the fourth amino acid residue, the Western quadrant is little explored for its SAR features to date.

The biosynthesis of the apratoxins is predicted to be initiated by a polyketide synthase (PKS1) section which transitions into the NRPS-encoded amino acid portion (AA1 to AA5), interrupted by one short PKS module (PKS2), and terminates with a cyclization to form the final product.[19] Previously reported apratoxin analogues appear to result from altered methylation patterns (Apr B and C), alterations in the number of PKS modules (Apr D), or modifications to the PKS optional domains (Apr E). (Scheme 1) By contrast, the variations in amino acid composition that are represented by apratoxins F and G result from either alterations in the adenylation domains present in the NRPS genes, or promiscuity in the selected substrate by two of these adenylation domains.[26] For example, the geometrical constraints present in the adenylation specificity pockets encoding for Ile and Val are relatively similar,[27] and lack of substrate discrimination may explain this substitution in the penultimate residue of apratoxin F and G (AA 4). On the other hand, a substantial change in the amino acid residues at several positions is required to explain the conversion of a proline encoding A-domain specificity pocket into that specifying for an alanine residue.[28] Moreover, the apratoxin F and G pathways incorporate an *N*-methyl group at this terminal residue position; either this is a newly incorporated enzymatic feature in this final module, or it is present but not functional in the apratoxin A pathway due to adenylation specificity for proline. Thus, it appears that this terminal portion of the apratoxin pathway has been modified to the greatest degree when comparing these two geographically divergent populations of *L. bouillonii*. Sequencing of this section of the biosynthetic clusters encoding for apratoxin A and F would be informative as to whether these modifications have arisen through mutations to this section of the cluster, through A-domain swapping via horizontal gene transfer and recombination events, and whether the *N*-methyl transferase is present in both pathways but only functional in those encoding for apratoxin F and G biosynthesis. Ultimately, comparison of these clusters will give keen insight into the evolution and diversification of this family of metabolites.

To gain some initial insight into the phylogenetic relationships of these different apratoxin-producing strains of *L. bouillonii*, a tree based on the SSU (16S) rRNA gene revealed a shared evolutionary history with other marine *Lyngbya* species (Figure 4) and, thus, supported the morphology-based taxonomic characterization above. (For a more detailed phylogenetic tree refer to supporting information) However, two different copies of the 16S rRNA gene were obtained from the apratoxin F and G producer, with 0.3% sequence divergence between the two copies. Secondary structure modelling pinpointed the nucleotide substitutions between these two copies as compensatory base changes (CBC) positioned at lagging helix strands of the RNA molecules. Based on the conserved nature of the RNA molecule the gene variations were assumed to correspond to different ribosomal operons in the *Lyngbya* genome.[29]

To gain further insight into the phylogenetic differences between this new chemotype and other apratoxin-producing *L. bouillonii* strains, a multi locus sequencing typing (MLST) comparison was performed with an apratoxin A-C producer from Papua New Guinea. Three common house-keeping genes composed of: (i) the 16S rRNA gene, (ii) the 16S-23S internal transcribed spacer (ITS) intergenic region, (iii) and the RNA polymerase γ-subunit (rpoC1) encoded gene were analyzed. Phylogenetic- and BLAST-analysis of each house-keeping gene supported the overall phylogenetic relatedness obtained from the 16S rRNA gene. (Figure 4) In accordance with the ribosomal genes, the 16S–23S ITS-regions were also obtained in two variable copies per genome. The four ITS-regions shared an average gene sequence identity of 89.7% within the genomes and 90.5% between the two apratoxin chemotypes. The rpoC1 gene was only found as a single-copy gene when sequencing four clones per gene library. The rpoC1 gene varied with 3.2% between the two *L. bouillonii* chemotypes. Unfortunately, there are an insufficient number of rpoC1 gene sequences in public data bases to fully explore the evolutionary histories and relationships between these different apratoxin-producers, but this gene robustly distinguishes these two strains from one another. Therefore, for future comparisons we strongly encourage the description of novel cyanobacterial chemotypes by multiple house-keeping genes, especially those influenced by different evolutionary pressures and structural constraints, such as RNA-encoded genes, protein-encoded genes, and intergenic regions.

Conclusion

In conclusion, apratoxins F and G represent two highly interesting analogs of the apratoxin family for a variety of reasons. They are the first analogs which posses significant alterations of the amino acid composition in the peptidic portion of the apratoxin skeleton. Secondly, these new apratoxins retain potent cancer cell cytotoxicity despite these alterations in constituent amino acids, thus revealing a previously unrecognized site of potential structural tolerance in the apratoxin family of cancer cell toxins. Thirdly, the producing organism was collected from a location very distant from previous collections of *L. bouillonii*, and there was no evidence of any of the other known apratoxin analogs present in its extracts. Thus, it appears that the apratoxin biosynthetic gene cluster has evolved between these two geographically distinct populations of *Lyngbya bouillonii*, presumably in response to differing environmental pressures, so as to diversify the suite of its cytotoxic natural products. Finally, our demonstration of in vivo antitumor effects for apratoxin A (**1**) validates our in vitro clonogenic assay approach to drug dosing, and enhances interest in the apratoxins as antineoplastic drug lead.

Experimental Section

General Experimental Procedures

Optical rotations were measured with a JASCO P-2000 polarimeter. UV spectra were measured on a Beckman Coulter DU-800 spectrophotometer while IR spectra were recorded on a Nicolet IR 100 FT-IR spectrophotometer. NMR spectra were acquired on a Varian Inova 600 MHz spectrometer and referenced to residual solvent ^{1}H and ^{13}C signals (δH 7.26, δC 77.0 for $CDCl_3$). Low-resolution ESI-MS were acquired on a Finnigan LCQ Advantage Max mass spectrometer, while high-accuracy mass measurements were obtained on an Agilent ESI-TOF mass spectrometer. Purification of the compounds was carried out on a Waters HPLC system equipped with a Waters 515 binary pump and a Waters 996 PDA detector.

Biological Material Collection and Identification

The marine cyanobacterium *Lyngbya bouillonii* PAL08-16 was collected from a depth of 9–15 m from Palmyra Atoll (N 05°52.021, W 162°03.262) using SCUBA. The samples were stored in 1:1 EtOH/H_2O and frozen at −20 °C. Specimens for genetic analysis (~200 mg) were preserved in RNA*later*® (10 mL) (Ambion Inc., Austin, TX, USA). A voucher specimen is available from WHG as collection number PAL 08-16-08-3.

Morphological Characterization

Morphological characterizations were performed using an Olympus IX51 epifluorescent microscope (100X) equipped with an Olympus U-CMAD3 camera. Measurements were provided as: mean ± standard deviation (SD). The filament means were the average of three filament measurements and cell measurements the average of ten adjacent cells of three filaments. Taxonomic identification of cyanobacterial specimens was performed in accordance with modern taxonomic systems.[30, 31]

DNA Extraction, PCR and Cloning

Genomic DNA was extracted from ~40 mg of cleaned cyanobacterial filaments using the Wizard® Genomic DNA Purification Kit (Promega) following the manufacturer's specifications. The isolated DNA was further purified using a Genomic-tip 20/G kit (Qiagen). DNA concentration and purity was measured on a DU® 800 spectrophotometer (Beckman Coulter) at a 1:10 dilution. The 16S rRNA genes were PCR-amplified using the cyanobacterial-specific primers 106F and 1509R,[32] the *rpoC1* genes using the degenerate primers LrpoC1-F and LrpoC1-R,[29] and the 16S-23 ITS region using 320–340 primers.[33] The PCR reaction volumes were 25 μL containing DNA (0.5 μL, ~50 ng), 10 x PfuUltra IV reaction buffer (2.5 μL), dNTP mix (0.5 μL, 25 mM)), each primer (0.5 μL, 10 μM), PfuUltra IV fusion HS DNA polymerase (0.5 μL) and dH_2O (20.5 μL). The PCR reactions were performed in an Eppendorf® Mastercycler® gradient as follows: initial denaturation for 2 min at 95°C, 25 cycles of amplification: 20 sec at 95°C, 20 sec at 50°C and 1.5 min at 72°C, and final elongation for 3 min at 72°C. PCR-products were analyzed on a (1%) agarose-gel in SB-buffer and visualized by EtBr-staining. PCR products were subcloned using the Zero Blunt® TOPO® PCR Cloning Kit (Invitrogen) into the pCR®-Blunt IV TOPO® vector, and then transformed into TOPO® cells and cultured on LB-kanamycin plates. Plasmid DNA was isolated using the QIAprep® Spin Miniprep Kit (Qiagen) and sequenced with M13F/M13R primers. Sequencing of the 16S rRNA genes' middle regions were improved using the internal primers 359F and 781R.[32] The gene sequences are available in the DDBJ/EMBL/GenBank databases under the following acc. No.: 16S rRNA gene (*rrn* A: GU111927; *rrn* B: GU182894), *rpoC1* (GU111928), and 16S-23 *ITS* (*rrn* A: GU111929; *rrn* B: GU111926).

Phylogenetic Inference

All gene sequences were aligned using ClustalW XXL in MEGA 4.0 with standard gap opening and extension penalties without gaps.[34] The secondary RNA structures were predicted by CLC Combined Workbench 3.5.2 (CLC bio, Cambridge, MA, USA). Mutation types and domains of the 16S rRNA genes were determined by superimposing their secondary structures on the SSU model for *Escherichia coli* J01695.[35] The evolutionary histories of the cyanobacterial genes were inferred using Maximum likelihood (ML), Maximum Parsimony (MP) and Bayesian inference algorithms. Appropriate nucleotide substitution models were selected using Akaike information criterion (AIC) and Bayesian information criterion (BIC) in Modeltest 3.7.[36] The Maximum likelihood (ML) inference was performed using PhyML v2.4.4.[37] The analysis was run using the GTR+I+G model (selected by AIC and BIC criteria) assuming a heterogeneous substitution rates and gamma

substitution of variable sites (proportion of invariable sites (pINV) = 0.419, shape parameter (α) = 0.414, number of rate categories = 4). Bootstrap resampling was performed on 500 replicates. Bayesian analysis was conducted using MrBayes 3.1.[38] The Bayesian inference was performed using the GTR+I+G substitution model (pINV = 0.450, α = 0.449, number of rate categories = 4) with Markov chains (one cold and three heated) ran for 3,000,000 generations. The first 25% were discarded as burn-in and the following data set were being sampled with a frequency of every 100 generations. The MP inference was run using the Maximum Composite Likelihood method. The MP tree was searched using the Close-Neighbor-Interchange (CNI) algorithm at a search level of 1.[39] All positions containing gaps and missing data were eliminated from the dataset (Complete deletion option) for a total of 1372 bp (~95% of the gene coverage).

Extraction and Isolation

L. bouillonii 142.9 g (dry wt) was extracted five times with 2:1 CH_2Cl_2/MeOH and concentrated to dryness in vacuo to give 4.3 g of crude extract. A portion of the crude extract (2.6 g) was subjected to VLC chromatography using a gradient of 0–100% EtOAc in hexanes followed by 0–100% gradient of MeOH in EtOAc to yield nine fractions (A–I). Fraction G [eluted with 100% EtOAc (21.7 mg)], Fraction H [eluted with 50% MeOH in EtOAc (170.4 mg)], and Fraction I [eluted with 100% MeOH (377.7 mg)] showed potent toxicity against brine shrimp and H-460 lung cancer cells. A portion of fraction H (31.5 mg) was further purified by sequential isocratic RP HPLCs [100% MeOH (Synergi 10u Fusion RP 250×10; 2 mL/min) followed by 85:15 CH_3CN/H_20 (Synergi Fusion 4μ; 2 mL/min)] to give 6.6 mg of apratoxin F and 0.4 mg of apratoxin G as amorphous powders.

Apratoxin F (**6**): amorphous powder $[\alpha]_D$ = −250 (*c* 0.33, CH_3CN); UV (MeOH) λ_{max} (log ε) 204 (6.52), 226 (6.33), 282 (5.27) nm; IR (film) ν max 3423 (br), 2963, 1740, 1621, 1511, 1460, 1387, 1247, 1182, 1088 cm-1; ^1H and ^{13}C NMR, see Table 1; ESIMS obs. *m/z* 828.32, 872.92; HR-ESIMS *m/z* 850.4800 (calcd for $C_{44}H_{69}N_5O_8SNa$, 850.4765).

Apratoxin G (**7**): amorphous powder $[\alpha]_D$ = −206 (*c* 0.02, ACN); UV (MeOH) λ_{max} (log ε) 204 (6.30), 226 (6.06), 282 (5.07) nm; IR (film) νmax 3423 (br), 2963, 1740, 1621, 1511, 1460, 1387, 1247, 1182, 1088 cm-1; ^1H and ^{13}C NMR, see Table 1; ESIMS *m/z* 814.30, 859.91; HR-ESIMS *m/z* 814.4782 (calcd for $C_{43}H_{68}N_5O_8S$, 814.4783).

Hydrolysis and Marfey's Analysis

Samples of **6** (0.5 mg, 0.0006 mmol) and **7** (0.5 mg, 0.0006 mmol) were separately treated with 6 N HCl in sealed vials at 120 °C for 24 h. The solutions were concentrated to dryness under a stream of N_2. The dried hydrolysates were then treated with a solution of FDAA (0.25 mg, 0.0009 mmol) in acetone (50 μL) and 0.1 M $NaHCO_3$ (100 μL) and heated to 90 °C for 5 min in sealed vials. The reaction was neutralized with 2 N HCl (50 μL) and diluted with CH_3CN (100 μL). The resulting solutions were then analyzed by RP-HPLC-MS using a LiChrosphere C18 column (125 × 4 mm) and a gradient of 15%CH_3CN:85% acidified H_2O (0.1% HCOOH) to 40% CH_3CN:60% acidified H_2O (0.1 % HCOOH) over 45 min at 0.8 mL/min, and monitored using a PDA detector as well as mass. Amino acid standards for chromatographic comparison were treated in identical fashion.

Biological Activity

Brine shrimp (*Artemia salina*) toxicity was measured as previously described.[22] After a 24 h hatching period, aliquots of 10 mg/mL stock solutions of sample were added to test wells containing 5 mL of artificial seawater and brine shrimp to achieve a final range of concentrations from 1 to 100 ppm. After 24 h the live and dead shrimp were tallied.

Cytotoxicity was measured in NCI H-460 human lung tumor cells with cell viability being determined by MTT reduction.[23] Cells were seeded in 96-well plates at 6000 cells/well in 180 μL of medium. After 24 h, the test chemicals were dissolved in DMSO and diluted into medium without fetal bovine serum and then added at 20 μg/well. DMSO was less than 0.5% of the final concentration. After 48 h, the medium was removed and cell viability determined.

Cytotoxicity was measured in HCT-116 cells using a hemocytometer. These cells were grown in 5 mL culture medium (RPMI-1640 + 15% FBS containing 1% penicillin-streptomycin and 1% glutamine) at 37 °C and 5% CO_2 at a starting concentration of 5×10^4 cells/T25 flask. On day 3, cells were exposed to different concentrations of the drug. Flasks were incubated for 120 h (5 days) in a 5% CO_2 incubator at 37 °C, and the cells were harvested with trypsin, washed once with HBSS, and then resuspended in HBSS and counted using a hemocytometer. The results were normalized to an untreated control and IC_{50} values determined using Excel.

Clonogenic concentration- and time-survival studies were carried out with HCT-116. These cells were grown in 5 mL culture medium (RPMI-1640 + 15% FBS containing 1% penicillin-streptomycin and 1% glutamine) at 37 °C and 5% CO_2 at a starting cell density of 5×10^4 cells/T25 flask. On day 3, cells were exposed to different concentrations of the drug. Apratoxin A (**1**) or F (**6**) was added to the medium (RPMI + 10% FBS) to a final concentration of 1 μg/mL (1.2 μM) and 10-fold dilutions thereof. At either 2 or 24 h, the cells were removed, washed and seeded at 200 or 20,000 cells in 60 mm dishes. For continuous exposure to drug, the medium containing the compounds remained in contact with the cells for the entire incubation period (168 h). The dishes were incubated for 7 days, the medium was removed, and the colonies were stained with methylene blue. Colonies containing 50 cells or more were counted. The results were normalized to an untreated control. Plating efficiency for the untreated cells was about 90%.

In vivo Evaluation of Apratoxin A (1)

Individual body weights for test mice were within 5 g of one another, and all mice were over 17 g at the start of drug therapy. The mice were supplied food and water ad libitum. The animals were pooled, implanted subcutaneously with tumor cells, and pooled again before distribution to treatment and control groups. Drug treatment was started three days after tumor inoculation, and intravenous administrations were given as 0.25 mL volumes via the tail vein. Tumor weights were estimated from 2-dimensional caliper measurements performed twice a week [tumor weight (mg) = $(a \times b^2)/2$ (where a and b are the tumor length and width, respectively, in mm)].The %T/C value was measured when the median control group tumor had reached a size of about 1000–1200 mg. The median tumor weight of both groups (T=treated, C= control) was determined, including a value of zero for non-detectable tumor masses. The %T/C is an indication of antitumor effectiveness; at values equal to or less than 42%, the compound is considered to demonstrate good antitumor activity. At a %T/C less than 10%, a compound is considered to possess highly significant antitumor activity, and is the level used by the NCI to justify a clinical trial if toxicity, formulation and other requirements are met (termed DN-2 level activity). A weight loss nadir of greater than 20% (mean of group) or greater than 20% drug deaths are considered to be an excessively toxic dose. The methods of tumor transplantation, protocol design, drug treatment, definition of terms and data analysis have been published.[40]

Acknowledgments

We thank the Palmyra Atoll Research Consortium for permitting sample collections on Palmyra Atoll and R. C. Coates for help in the collection of these materials. We further gratefull acknowledge the government of Papua

New Guinea for permission to collect apratoxin A producing strains of L. bouillonii. We also acknowledge The Growth Regulation & Oncogenesis Training Grant NIH/NCI (T32CA009523-24) for a fellowship to K. T. and NIH/NCI CA100851 for funding this research.

References

1. Dewick, PM. Medicinal Natural Products: A Biosynthetic Approach. Wiley; West Sussex, UK: 2009. p. 539
2. Tan LT. Phytochemistry. 2007; 68:954–79. [PubMed: 17336349]
3. Tidgewell, K.; Clark, BR.; Gerwick, WH. The Natural Products Chemistry of Cyanobacteria. In: Moore, B.; Crews, P., editors. Comprehensive Natural Products Chemistry. 2. Elsevier; Oxford: 2010.
4. Luesch H, Yoshida WY, Moore RE, Paul VJ, Corbett TH. J Am Chem Soc. 2001; 123:5418–23. [PubMed: 11389621]
5. Luesch H, Yoshida WY, Moore RE, Paul VJ. Bioorg Med Chem. 2002; 10:1973–8. [PubMed: 11937357]
6. Gutierrez M, Suyama TL, Engene N, Wingerd JS, Matainaho T, Gerwick WH. J Nat Prod. 2008; 71:1099–103. [PubMed: 18444683]
7. Matthew S, Schupp PJ, Luesch H. J Nat Prod. 2008; 71:1113–6. [PubMed: 18461997]
8. Chen J, Forsyth CJ. J Am Chem Soc. 2003; 125:8734–5. [PubMed: 12862462]
9. Chen J, Forsyth CJ. Proc Natl Acad Sci USA. 2004; 101:12067–72. [PubMed: 15231999]
10. Doi T, Numajiri Y, Munakata A, Takahashi T. Org Lett. 2006; 8:531–4. [PubMed: 16435877]
11. Ma D, Zou B, Cai G, Hu X, Liu JO. Chem Eur J. 2006; 12:7615–26. [PubMed: 16832801]
12. Numajiri Y, Takahashi T, Doi T. Chem Asian J. 2009; 4:111–25. [PubMed: 19034894]
13. Chen J, Forsyth CJ. Org Lett. 2003; 5:1281–3. [PubMed: 12688739]
14. Zou B, Wei J, Cai G, Ma D. Org Lett. 2003; 5:3503–6. [PubMed: 12967310]
15. Gilles A, Martinez J, Cavelier F. J Org Chem. 2009; 74:4298–304. [PubMed: 19432410]
16. Luesch H, Chanda SK, Raya RM, DeJesus PD, Orth AP, Walker JR, Izpisua Belmonte JC, Schultz PG. Nat Chem Biol. 2006; 2:158–67. [PubMed: 16474387]
17. Liu Y, Law BK, Luesch H. Mol Pharmacol. 2009; 76:91–104. [PubMed: 19403701]
18. Shen S, Zhang P, Lovchik MA, Li Y, Tang L, Chen Z, Zeng R, Ma D, Yuan J, Yu Q. J Cell Biol. 2009; 185:629–39. [PubMed: 19433452]
19. Grindberg, RV. PhD Thesis. University of California; San Diego: 2009.
20. Gu L, Wang B, Kulkarni A, Geders TW, Grindberg RV, Gerwick L, Hakansson K, Wipf P, Smith JL, Gerwick WH, Sherman DH. Nature. 2009; 459:731–5. [PubMed: 19494914]
21. Hoffmann L, Demoulin V. Belg J Bot. 1991; 124:82–8.
22. Meyer BN, Ferrigni NR, Putnam LB, Jacobsen LB, Nichols DE, McLaughlin JL. Planta Med. 1982; 45:31–33.
23. Manger RL, Leja LS, Lee SY, Hungerford JM, Hokama Y, Dickey RW, Granade HR, Lewis R, Yasumoto T, Wekell MM. J AOAC Int. 1995; 78:521–27. [PubMed: 7756868]
24. Subramanian B, Nakeff A, Tenney K, Crews P, Gunatilaka L, Valeriote FV. J Exp Ther Oncol. 2006; 5:195–204. [PubMed: 16528970]
25. Polin L, Valeriote F, White K, Panchapor C, Pugh S, Knight J, LoRusso P, Hussain M, Liversidge E, Peltier N, Golakoti T, Patterson G, Moore R, Corbett TH. Invest New Drugs. 1997; 15:99–108. [PubMed: 9220288]
26. Hoffmann D, Hevel JM, Moore RE, Moore BS. Gene. 2003; 311:171–80. [PubMed: 12853152]
27. Challis GL, Ravel J, Townsend CA. Chemistry & Biology. 2000; 7:211–24. [PubMed: 10712928]
28. Stachelhaus T, Mootz HD, Marahiel MA. Chemistry & Bilogy. 1999; 6:493–505.
29. Engene N, Coates RC, Gerwick WH. J Phycol. 2010 in press.
30. Castenholz RW, Norris TB. Algological Studies. 2005; 117:53–69.

31. Komarek, J.; Anagnostidis, K. Cyanoprokaryota -2nd Part: Oscillatoriales. In: Büdel, B.; Krienitz, L.; Gärtner, G.; Schagerl, M., editors. Süsswasserflora von Mitteleuropa. Vol. 19/2. Elsevier/ Spektrum; Heidelberg: 2005.
32. Nubel U, Garcia-Pichel F, Muyzer G. Appl Environ Microbiol. 1997; 63:3327–32. [PubMed: 9251225]
33. Iteman I, Rippka R, De Marsac NT, Herdman M. Microbiology. 2000; 146:1275–86. [PubMed: 10846207]
34. Tamura K, Dudley J, Nei M, Kumar S. Mol Biol Evol. 2007; 24:1596–9. [PubMed: 17488738]
35. Cannone JJ, Subramanin S, Schnare MN, Collett JR, D'Souza LM, Du Y, Feng B, Lin N, Madabusi LV, Muller KM, Pnde N, Schang Z, Yu N, Gutell RR. BMC Bioinformatics. 2002; 3:1471–2105.
36. Posada D, Crandall KA. Bioinformatics. 1998; 14:817–8. [PubMed: 9918953]
37. Guindon S, Gascuel O. System Biol. 2003; 52:696–704. 2003. [PubMed: 14530136]
38. Ronquist F, Huelsenbeck JP. 2003; 12:1572–4.
39. Nei, M.; Kumar, S. Molecular Evolution and Phylogenetics. Oxford University Press; New York: 2000.
40. Corbett T, Valeriote F, LoRusso P, Polin L, Panchapor C, Pugh S, White K, Knight J, Demchik L, Jones J, Jones L, Lowichik N. Int J Pharm. 1995; 33:102–22.

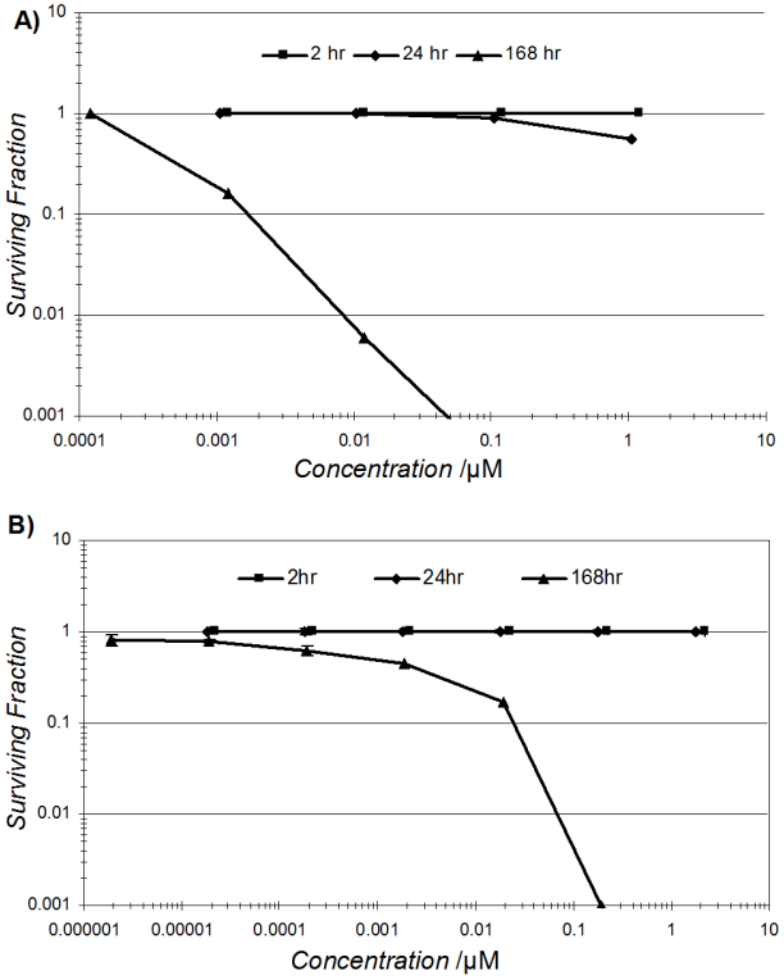

Figure 1.
Clonogenic Dose Response of **A)** apratoxin A and **B)** apratoxin F in HCT-116 cells

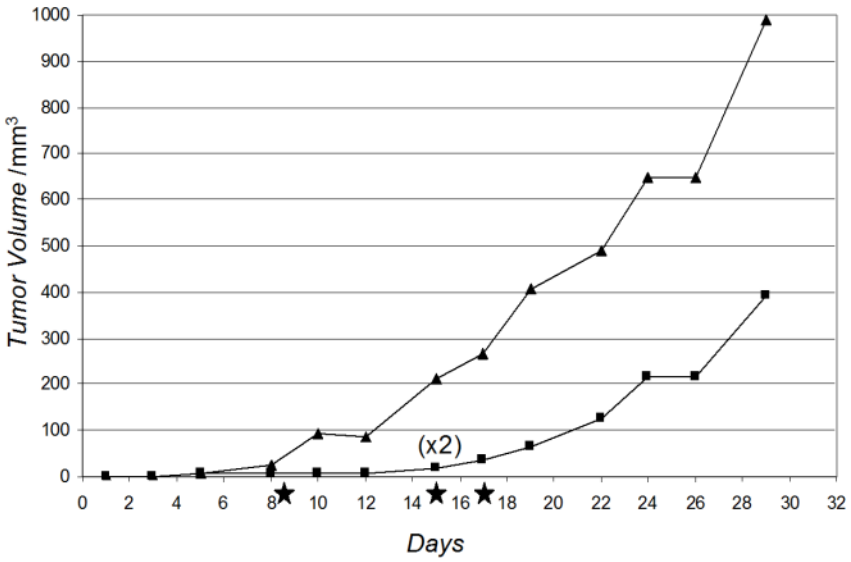

Figure 2.
Tumor Size versus day post implantation. Control (▲) and 0.0125 mg/mouse Apratoxin A (■). ★animals were found dead on these days

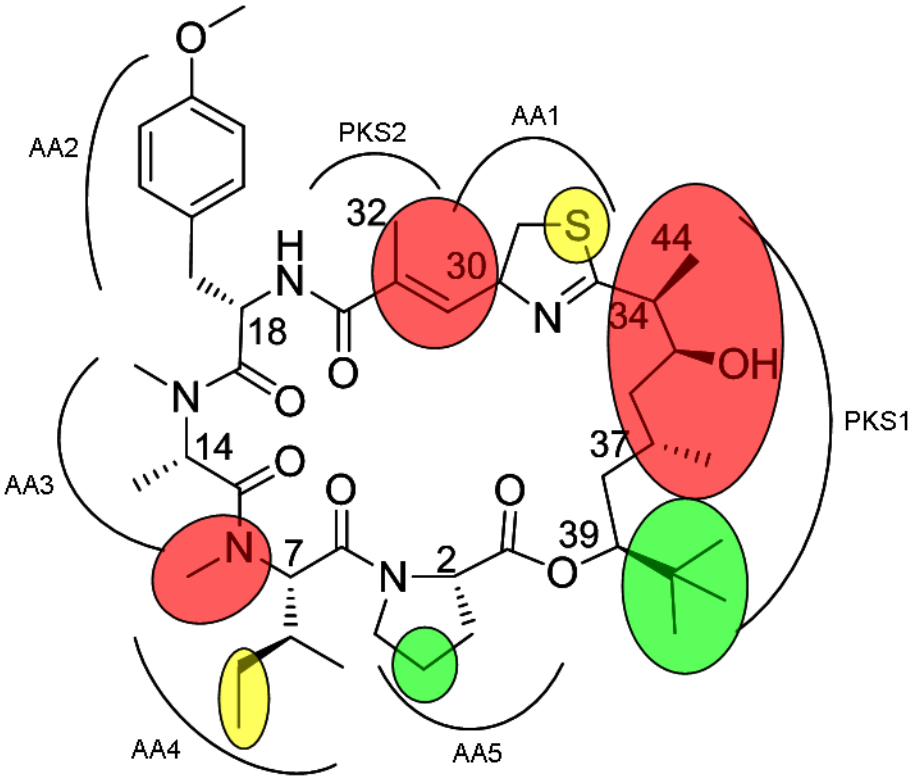

Figure 3.
SAR of the Apratoxin Core for Cytotoxicity. (Red – Alteration not tolerated, Yellow – Alteration has minor affect on activity, Green – Modification allowed.)

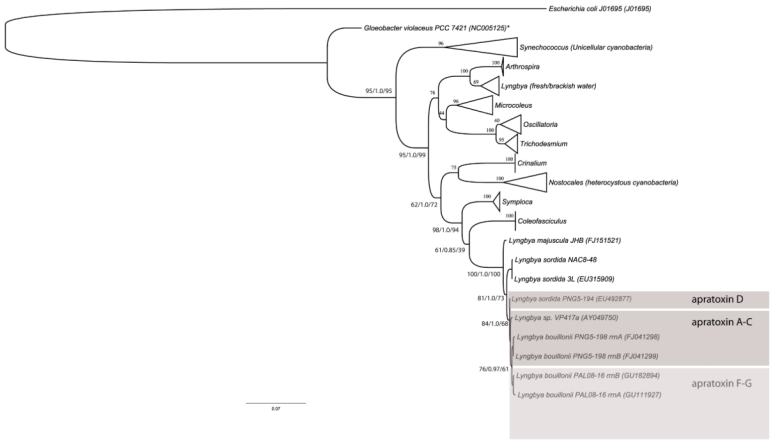

Figure 4.

Maximum-likelihood (PhyML) phylogenetic tree of the apratoxin F–G producer *Lyngbya bouillonii* PAL08-16 with other apratoxin-producing strains and marine *Lyngbya* species based on 16S sequence. *Escherichia coli* J01695 and *Gloeobacter violaceus* PCC 7421 were used as outgroups and type strains of the cyanobacterial lineages: *Trichodesmium*, *Oscillatoria*, *Microcoleus*, *Planktothrix*, *Symploca*, *Geitlerinema*, *Limnothrix* and *Leptolyngbya* were added to enhance the evolutionary perspective. The support values at important nodes are indicated as boot-strap (ML), posterior probability (MrBayes) and boot-strap (MP). Specimens are designated as taxa, strain and acc. Nr. in brackets.

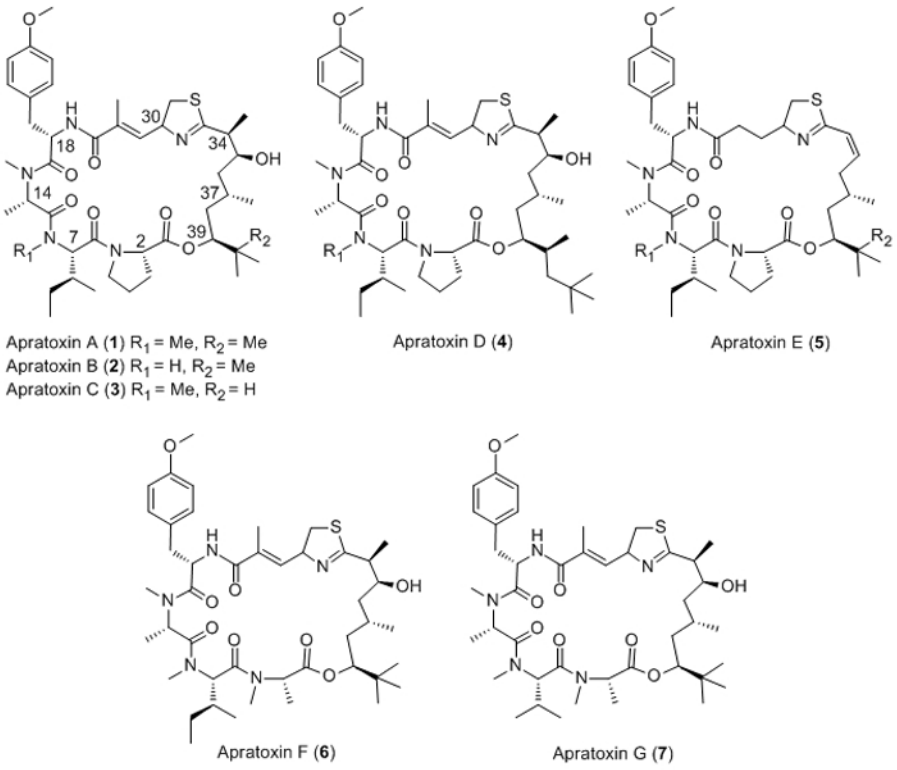

Scheme 1.
Apratoxins A–E (**1**–**5**), Apratoxin F (**6**), and Apratoxin G (**7**)

Table 1

NMR Spectroscopic Data (600 MHz, $CDCl_3$) for Apratoxin F (**6**) and Apratoxin G (**7**)

	Apratoxin F (6)				Apratoxin G (7)		
	δC, mult	**δH, (*J* in Hz)**	**HMBC**		**δC, mult**	**δH, (*J* in Hz)**	**HMBC**
NMeAla				NMeAla			
1	173.6, qC			1	173.3, qC		
2	54.4, CH	4.47 d(7.2)	1, 3, 5	2	54.3, CH	4.46 q(7.8)	1, 3, 5, 6
3	14.8, CH_3	1.44 d(7.8)	2	3	15.0, CH_3	1.43 d(7.8)	1, 2
5	31.1, CH_3	3.27 s	1, 2, 6	5	31.2, CH_3	3.28 s	2, 3, 6
NMeIle				NMeVal			
6	173.0, qC			6	173.7, qC		
7	54.8, CH	5.48 d(11.4)	5, 6, 8, 9, 11, 12, 13	7	58.0, CH	5.26 d(11.4)	6, 8, 9, 12, 13
8	31.7, CH	2.26 m	7, 10, 11	8	27.5, CH	2.22 m	7, 9, 10
9a	24.6, CH_2	0.96 m	7, 8, 10	9	19.7, CH_3	0.95 d(6.6)	7, 8, 10
9b		1.3 m	7, 8, 10				
10	8.8, CH_3	0.89 s	9	10	18.9, CH_3	0.72 d(6.0)	7, 8, 9
11	13.9, CH_3	0.92 d (6.6)	7, 8				
12	30.4, CH_3	2.68 s	7, 13	12	30.3, CH_3	2.66 s	7, 13
NMeAla				NMeAla			
13	170.0, qC			13	170.4, qC		
14	60.6, CH	3.28 m	15	14	60.5, CH	3.28 m	
15	14.1, CH_3	1.22 d(6.6)	13, 14	15	14.1, CH_3	1.18 d(6.6)	13, 14
16	36.7, CH_3	2.79 s	13, 14, 17	16	36.9, CH_3	2.80 s	13, 14, 17
OMeTyr				OMeTyr			
17	170.4, qC			17	170.6, qC		
18	50.5, CH	5.05 dd(4.8, 10.2, 10.2)	17, 19, 27	18	50.4, CH	5.04 ddd(4.8, 10.2, 10.2)	17, 19, 20, 27
19a	37.2, CH_2	2.87 dd(4.8, 12.6)	17, 18, 20, 21, 25	19a	37.5, CH_2	2.88 dd(4.8, 12.0)	17, 18, 20, 21, 25
19b		3.10 d(11.4)	17, 18, 20, 21, 25	19b		3.07 dd(12.0, 12.0)	17, 18, 20, 21, 25
20	128.2, qC			20	128.2, qC		
21/25	130.6, CH	7.16 d(8.4)	19, 20, 22, 23, 24	21/25	130.6, CH	7.14 d(8.4)	19, 22, 23, 24

	Apratoxin F (6)			Apratoxin G (7)			
	δC, mult	**δH, (*J* in Hz)**	**HMBC**		**δC, mult**	**δH, (*J* in Hz)**	**HMBC**
22/24	113.9, CH	6.8 d(9.0)	20, 21, 23, 25	22/24	114.0, CH	6.80 d(9.0)	20, 23
23	158.6, qC			23	158.9, qC		
26	55.3, CH_3	3.78 s	23	26	55.3, CH_3	3.78 s	23
NH		6.07 d(9.6)	27	NH		6.13 d(9.0)	18, 27
MoCys				MoCys			
27	169.5, qC			27	169.6, qC		
28	130.6, qC			28	130.2, qC		
29	136.2, CH	6.37 d(9.0)	27, 31, 32	29	136.4, CH	6.44 d(9.6)	27, 28, 31, 32
30	72.4, CH	5.25 ddd(4.2, 9.3, 9.3)	28, 29, 33	30	72.4, CH	5.27 ddd(4.2, 9.6, 9.6)	28, 29, 33
31a	37.6, CH_2	3.15 dd(4.2, 4.2)	29, 30, 33	31a	37.7, CH_2	3.17 dd(3.6, 10.8)	29, 30, 33
31b		3.46 dd(8.4, 11.1)	29, 30	31b		3.47 dd(8.7, 11.1)	29, 30
32	13.3, CH_3	1.97 s	27, 28, 29	32	13.3, CH_3	1.98 s	27, 28, 29
Polyketide				Polyketide			
33	177.3, qC			33	177.8, qC		
34	48.8, CH	2.64 dd(7.2, 10.2)	33, 35, 44	34	48.8, CH	2.63 dd(7.2, 10.2)	33, 35, 44
35	71.7, CH	3.56 dddd(3.0, 10.5, 10.6, 10.6)		35	71.8, CH	3.54 dddd(2.4, 10.6, 10.8, 10.8)	
36a	38.3, CH_2	1.11 m	45	36a	38.5, CH_2	1.11 m	45
36b		1.47 m	34, 35, 37, 45	36b		1.47 m	34, 35, 37, 45
37	24.3, CH	2.14 m		37	24.4, CH	2.13 m	
38a	37.7, CH_2	1.26 m	37, 45	38a	37.5, CH_2	1.25 m	37
38b		1.79 ddd(2.4, 13.2, 13.2)	37, 39	38b		1.78 ddd(3.0, 12.6, 12.6)	37, 39, 45
39	77.2, CH	4.88 dd(1.8, 12.6)	1, 40, 41, 42, 43	39	77.3, CH	4.88 dd(2.4, 12.6)	1, 38, 40, 41, 42, 43
40	34.9, qC			40	35.0, qC		
41	26.1, CH_3	0.88 s	39, 40, 42, 43	41	26.2, CH_3	0.88 s	39, 40, 42, 43
42	26.1, CH_3	0.88 s	39, 40, 41, 43	42	26.2, CH_3	0.88 s	39, 40, 41, 43
43	26.1, CH_3	0.88 s	39, 40, 41, 42	43	26.2, CH_3	0.88 s	39, 40, 41, 42
44	16.7, CH_3	1.06 d(6.6)	33, 34, 35	44	16.6, CH_3	1.06 d(7.2)	30, 33, 34, 35
45	19.8, CH_3	1.00 d(6.6)	36, 37, 38, 39	45	19.0, CH_3	0.99 d(6.6)	36, 37, 38
OH		4.52 d(10.8)	35, 36	OH		4.51 d(10.8)	35, 36

Table 2

Zone Inhibition Assay

	µg/disk	L1210	Colon38	CFU- GM	HCT-116	H125	CEM
1	3.75	650	800	650	650	700	400
6	8.25	700	600	700	800	800	450